A Mathematical Model for Infiltration Heat Recovery

C. R. Buchanan and M. H. Sherman

Energy Performance of Buildings Group
Indoor Environment Department
Environmental Energy Technologies Division
Lawrence Berkeley National Laboratory
University of California

Abstract

Infiltration has traditionally been assumed to affect the energy load of a building by an amount equal to the product of the infiltration flow rate and the sensible enthalpy difference between inside and outside. However, laboratory and simulation research has indicated that heat transfer between the infiltrating air and walls may be substantial, reducing the impact of infiltration. In this paper, two- and three-dimensional CFD simulations are used to study the fundamental physics of the infiltration heat recovery process and a simple macro-scale mathematical model for the prediction of a heat recovery factor is developed. CFD results were found to compare well (within about 10 percent) with limited published laboratory data corresponding to one of the scenarios examined. The model, based on the steady-state one-dimensional convection-diffusion equation, provides a simple analytical solution for the heat recovery factor and requires only three inputs: the infiltration rate, the U-value for the building, and estimates of the effective areas for infiltration and exfiltration. The most difficult aspect of using the model is estimation of the effective areas, which is done here through comparison with the CFD results. With proper input, the model gives predictions that agree well with CFD results over a large range of infiltration rates. Results show that infiltration heat recovery can be a substantial effect and that the traditional method may greatly over-predict the infiltration energy load, by 80-95 percent at low leakage rates and by about 20 percent at high leakage rates. This model for infiltration heat recovery could easily be incorporated into whole-building energy analysis programs to help provide improved predictions of the energy impact of infiltration.

Nomenclature

a_i = dimensionless flow rate (-)
a_o = dimensionless flow rate based on total building surface area (-)
A = building envelope total surface area (m^2)
A_i = effective areas for heat recovery model (m^2)
e = external wall faces for conduction terms in model development
f_1 = effective area ratio for infiltrating wall (-)
f_2 = effective area ratio for exfiltrating wall (-)
k = thermal conductivity (0.025 W/m K)
L = wall thickness (m)

m = infiltration mass flow rate (kg/s)
Pe = Peclet number (-)
q_o = heat energy conducted through wall in model (W/m^2)
Q = actual total (conduction and convection) building energy load (W)
Q_{cond} = conduction energy flux through envelope in simplified model (W)
Q_{conv} = convection energy flux through envelope in simplified model (W)
Q_{inf} = actual energy load due to infiltration (W)
Q_{infC} = conventional energy load due to infiltration (W)
Q_o = pure conduction energy load with no infiltration (W)
T = temperature (K)
T_i = inside air temperature (298 K)
T_o = outside air temperature (274 K)
U = wall U-value (W/m^2)
ε = infiltration heat exchange effectiveness or heat recovery factor (-)
Γ = generic diffusion coefficient (kg/m s in this paper)

1. Introduction

Infiltration, accidental air leakage through building envelopes, is a common phenomenon that affects both indoor air quality and building energy consumption. Infiltration can contribute significantly to the overall heating or cooling load of a building, but the magnitude of the effect depends on a host of factors, including environmental conditions, building design and operation, and construction quality. A small number of studies regarding the energy issues of infiltration have been found in the literature. (4,9,10,11), and all concluded that the impact of infiltration can be sizeable.

$$Q_{infC} = mc_p(T_i - T_o) \qquad (1)$$

The conventional method of accounting for the extra load due to infiltration is to add a simple convective transport term of the form mc_pT to the energy balance for the building. For single-zone building models the conventional infiltration load, Q_{infC}, shown in equation 1, is the product of the infiltrating air mass flow rate, the specific heat capacity of air, and the temperature difference between inside and outside. This relation does not include the effects of moisture in the air and is strictly valid only if the leaking air does not interact thermally with the building walls. In reality, leaking air exchanges heat with the walls as it enters and leaves the building, which changes the thermal profile in the walls and warms or cools the infiltrating/exfiltrating air. This results in different values for the conduction, infiltration, and total heat losses than are predicted by the conventional method. Some studies have shown that this effect could be substantial suggesting that the conventional method over-predicts the energy impact of infiltration (1,2,5,6,7).

An improved prediction of the energy load due to infiltration can be made by introducing a correction factor, the infiltration heat exchange effectiveness, ε, or the heat recovery factor (defined by equation 2), into the expression for the conventional load

(equation 1). In equation 2, Q is the actual total energy load of the building with infiltration and Q_o is the conduction load when there is no infiltration. This heat recovery factor, introduced by Claridge and Bhattacharyya (6), accounts for the thermal interaction between leaking air and building walls. The actual infiltration load, Q_{inf}, is calculated using the heat recovery factor as shown in equation 3.

$$e \equiv 1 - \frac{Q - Q_o}{mc_p \Delta T} = 1 - \frac{Q - Q_o}{Q_{\text{inf } C}} \qquad (2)$$

$$Q_{\text{inf}} = (1 - e) mc_p (T_i - T_o) = (1 - e) Q_{\text{inf } C} \qquad (3)$$

2. Objectives and Problem Formulation

In this paper, two- and three-dimensional computational fluid dynamics (CFD) simulations are used to investigate the basic physics of the infiltration heat recovery process. We choose to start with a fairly simple physical representation (only conduction and convection are considered for transport) so that an understanding of the phenomenon can be developed from first principles. Additional processes, like turbulence or radiation, can be added progressively if necessary. Also, a one-dimensional mathematical model is developed that can be used to determine the extent of heat transfer between leaking air and walls, represented quantitatively as the infiltration heat recovery factor. This macro-scale model, based on the steady-state one-dimensional convection-diffusion equation, provides a simple analytical relation for the heat recovery factor. Predictions from the model are compared with results from detailed CFD simulations and limited experimental results from the literature.

The cross-section of a hypothetical test room under a general infiltration scenario is shown in figure 1. Small holes in the outer sheathing of the building envelope (plywood in this study) allow air to leak into the wall cavity and flow through the wall from outside to inside for the infiltrating wall and vice-versa for the exfiltrating wall. The driving force for leakage is a pressure differential due to wind and temperature differences between inside and outside. Four wall configurations, shown in figure 2, are examined under various environmental conditions. Wall geometries 1 and 2 have insulation in the wall cavity, while geometries 3 and 4 have empty wall cavities. Leakage rates through the wall are varied and the inside/outside temperature difference is fixed at 24 K.

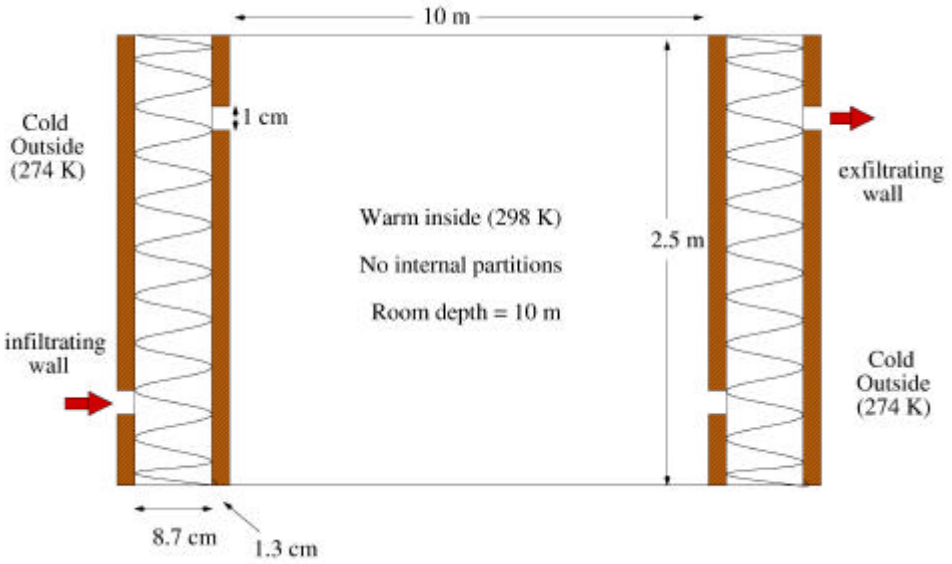

Figure 1: Cross-section of a hypothetical test room showing the general infiltration problem (wall geometry 1 shown). The infiltrating and exfiltrating walls have a conduction and convection energy flux, but all other walls have only a conduction flux.

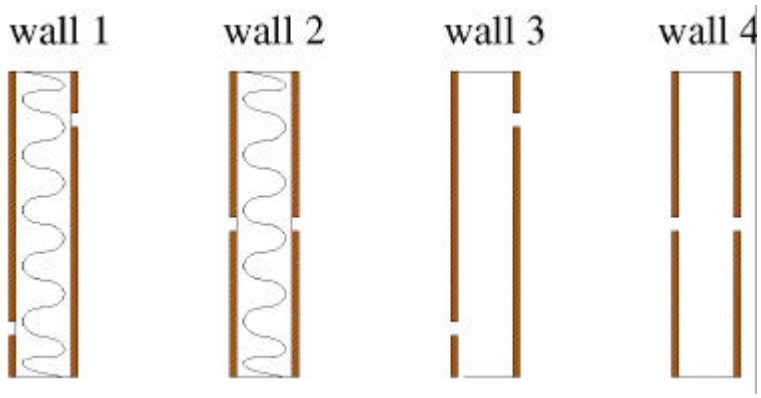

Figure 2: Wall geometries 1-4; 1 & 2 are insulated and 3 & 4 are empty.

3. CFD Simulations

In the first part of this study, computational fluid dynamics (CFD) simulations are used to examine the basic physics of the infiltration heat recovery process in detail. The individual contributions of conduction and convection to the total heating load are determined without making fundamental simplifications as in previous work (1,5,6). These components of the total energy flux are used to calculate the infiltration heat recovery factor.

The walls are modeled as two- and three-dimensional systems in the CFD simulations. Flow and energy transport in the air are determined via the Navier-Stokes and

energy equations. A laminar representation is used for the flow, and solutions show this to be a valid assumption, as the highest calculated Reynolds number inside or near the wall is only about 2000, based on wall thickness. It is possible that turbulence could have some effect even at these moderately low Reynolds numbers, so this will be examined in future work. The plywood sheathing is represented as an impermeable, solid material. Energy transport within the sheathing is calculated via the conduction equation. Insulation, if present in the wall, is represented as a porous material. Air flow through the insulation is determined via Darcy's Law, a common model for flow through porous media (3,7). Energy transport through the insulation is determined via a modified form of the energy equation, in which an effective conductivity is used in the conduction flux term and the thermal inertia of the solid component is included in the transient term. A fundamental assumption in the validity of this relationship for this application is local thermal equilibrium between the fluid and solid phases in the porous media. This assumption was tested and found to be accurate. The governing equations and other CFD issues are detailed in previous work by the authors (2).

3.1. CFD Results

Figure 3 shows the heat recovery factor for wall geometries 1-4 determined from two-dimensional CFD simulations. The variable on the horizontal axis of the graph is the dimensionless flow rate (a_o), defined in equation 4. It was found to be a useful independent variable when comparing the heat recovery for different cases because it collapses the data showing the universal trends. In all cases, the heat recovery factor approaches a value of one at very low flow rates and decreases with increasing flow rate. Heat transfer is lower at high flow rates because there is less time for energy to be transported from the walls to the infiltrating air resulting in lower heat recovery.

$$a_i = \frac{mc_p}{U_i A_i} \qquad (4)$$

Two distinct trends can be seen in figure 3. One trend is that the walls with holes in a high/low configuration, walls 1 and 3, have a significantly higher heat recovery factor than the walls with holes that are straight through. This is partly because the high/low configuration has a longer leakage path and, for a given flow rate, the air remains within the wall cavity for a longer period of time. This allows for greater heat transfer and higher heat recovery compared to the straight through case. However, these straight through geometries still show a significant heat recovery effect. The other trend is that data points for the high/low configurations fall roughly on a single trend line, and the same is true for the straight through configurations. That is, insulated (1 & 2) and empty walls (3 & 4) with the same hole configuration have about the same heat recovery when plotted against the chosen independent variable, a_o. This suggests a universal behavior that may be applicable to all leakage scenarios.

Three-dimensional simulations are performed for walls 1 and 2 and the results are shown in figures 5 and 6. The 3D simulations give nearly the same values and show the same trends for the heat recovery factor for a given hole configuration as the 2D simulations.

This suggests that it may be sufficient to use 2D simulations to study a given wall geometry, which means a large savings in time and effort compared to 3D simulations.

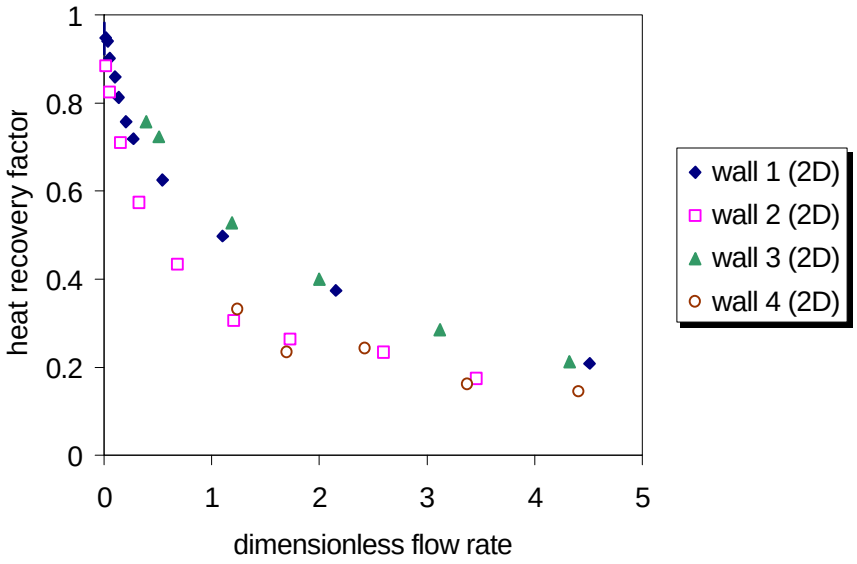

Figure 3: Heat recovery factor determined from 2D CFD simulations for walls 1-4. Solid symbols show data for walls with a high/low hole configuration (1 and 3) and hollow symbols show data for walls with a straight through hole configuration (2 and 4). Notice the two distinct trends—one for each hole configuration.

3.2. Experimental Comparison of CFD Results

The only experimental data available for comparison is that of Claridge and Bhattacharyya (6). Their case with a diffuse inlet and outlet (inlet B4, outlet A) is similar to walls 1 and 3 in this study (high/low hole configuration). They calculated a heat recovery factor of about 0.80 when a_o is 0.05 and about 0.65 when a_o is 0.25. As figure 3 shows, CFD results for wall 1 give a heat recovery factor of 0.90 when a_o is 0.05 and about 0.72 when a_o is 0.25. There are no CFD data available for wall 3 at these low flow rates, but the trend is the same. Considering the rough nature of the comparison, the experimental and CFD results show good agreement. There is only about a 10 percent discrepancy in the heat recovery factor at both points. This suggests that the CFD results are qualitatively, and, most likely, quantitatively accurate. Also, this suggests that processes which occur naturally in the experiment but that are not represented in the simulations (turbulence, radiation) may not have a strong effect on the heat recovery.

4. Development of the Simplified Infiltration Heat Recovery Model

In the following work, a simple macro-scale mathematical model is developed for the infiltration heat recovery factor. The model should provide a simple, yet accurate, means for calculating the heat recovery factor, ε, under a variety of environmental conditions, building designs, and leakage scenarios. The starting point is the steady-state one-dimensional convection-diffusion equation (12). This simple representation is used because we believe it includes the most important physical mechanisms and will help provide insight into the heat recovery process more easily than a complex representation. If the effect is sizeable and the topic merits further investigation, additions can be made to the model in future work, if necessary, to help provide more accurate, realistic results and to make it suitable for use in network codes.

4.1. Convection-Diffusion Equation

The one-dimensional convection-diffusion equation, shown in equation 5, represents transport by combined convection and diffusion in a steady flow varying in one spatial direction. ϕ represents any scalar flow variable, e.g., temperature or concentration, and Γ is the diffusion coefficient for that variable. An analytical solution is given by equation 6 for the variable ϕ as a function of the length coordinate x for r, u, and Γ constant and for prescribed boundary conditions and $x = 0$ and L. The subscripts 0 and L represent the bounds of the domain, i.e., the wall thickness, and the parameter Pe is the Peclet number, given by equation 7.

$$\frac{d}{dx}(ruf) = \frac{d}{dx}\Gamma\frac{df}{dx} \qquad (5)$$

$$\frac{f(x)-f_0}{f_L-f_0} = \frac{\exp(Pe\frac{x}{L})-1}{\exp(Pe)-1} \quad , \quad Pe = \frac{ruL}{\Gamma} \qquad (6),\ (7)$$

$$T(x) = T_0 + (T_L - T_0)\left(\frac{\exp(Pe\frac{x}{L})-1}{\exp(Pe)-1}\right) \qquad (8)$$

Taking f to be temperature, equation 6 can be rearranged to provide a simple relationship for the temperature at any location between the two bounds, as given by equation 8. This relationship will provide the basis for the heat recovery model. At this point, Γ is left as a generic diffusion coefficient. Later in the model development it will be given a prescribed value, via input, so that it takes on an effective value to represent the composite wall structure.

The next step is to apply equation 8 to a generic building envelope (shown in figure 4) under arbitrary conditions to determine the energy flux through the walls. Areas of the envelope that are affected by leaking air are represented by A1 and A2 (infiltrating and exfiltrating, respectively) and have both a convection and conduction energy flux. These sections represent parts of the wall in the vicinity of the leaking hole which undergo thermal changes due to infiltration and could potentially represent the entire infiltrating or exfiltrating walls. Areas that are not affected by leaking air are represented by A3 and A4 and have only conduction heat transfer. The six individual flux components shown in figure 4 are used to determine the infiltration heat recovery factor.

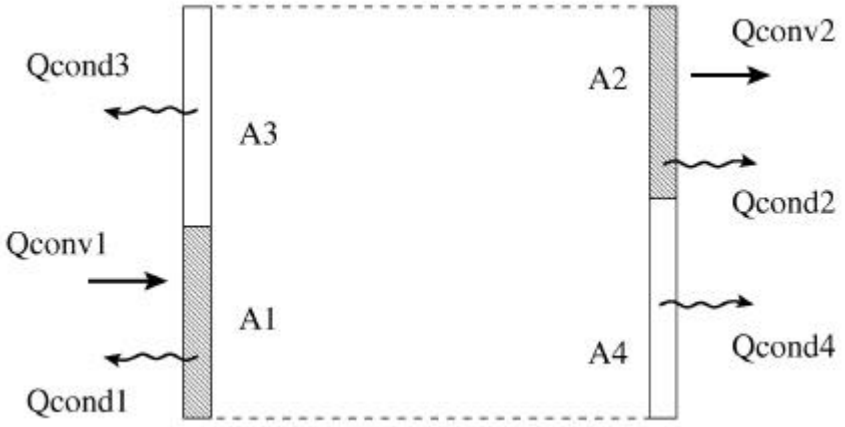

Figure 4: Energy flux through the simplified building envelope used in the model development. Sections A1 and A2 are affected by leaking air and have both convection and conduction terms. Sections A3 and A4 are not affected and have only a conduction term. The outer faces of the left and right walls form the system control volume boundary.

4.2. Convection Terms

The total energy flux through the building walls has two components, one due to convection (Q_{conv}) and another due to conduction (Q_{cond}). Each component will be determined across the control volume boundary via equation 8. There is a convection flux only through the two "effective" areas A1 and A2. These areas do not correspond to the physical area of a hole in the envelope, but to the surface area of the envelope that is affected by infiltrating air. The actual values for these effective areas, the only parameters not directly input into the model, will be estimated through comparison with CFD data.

$$Q_{conv} = Q_{conv2} - Q_{conv1} \quad (9)$$

$$Q_{conv} = mc_p T(x = L) - mc_p T(x = 0) \quad (10)$$

$$Q_{conv} = mc_p T_o - mc_p T_o \quad (11)$$

$$Q_{conv} = 0 \quad (12)$$

The net convective energy flux across the effective areas, A1 and A2, is determined in equations 9-12. Equation 9 states that the net convective flux is the flux at the exfiltrating wall minus the flux at the infiltrating wall, as shown in figure 4. Note, in this analysis, energy flow out of the building is considered positive. The air temperatures and mass flow rates at the control volume boundaries, i.e., the external face of the building envelope, are used in equation 10. The temperatures at the external boundaries are by definition the outside air temperature, as equation 11 reflects. Finally, equation 12 gives the interesting result that the net convective flux across the chosen control volume boundary is zero. Therefore, the total effective energy flux due to infiltration in the effective areas will be incorporated into the conduction terms.

4.3. Conduction Terms

The total conduction energy flux across the control volume boundary is given by equation 13. It states that the flux is equal to the dot product of the temperature gradient at the control volume boundary (the external wall faces, denoted by the subscript *e*) and an outward-pointing normal vector multiplied by the effective area and the wall thermal conductivity summed over the entire boundary. Equation 14 gives the expanded form of equation 13 when applied to the building envelope shown in figure 4.

$$Q_{cond} = \sum_{i=1}^{4} -k_i A_i \left(\nabla T \bullet \hat{n}\right)\Big|_{e,i} \quad (13)$$

$$Q_{cond} = k_1 A_1 \left.\frac{dT}{dx}\right|_{e,1} - k_2 A_2 \left.\frac{dT}{dx}\right|_{e,2} + k_3 A_3 \left.\frac{dT}{dx}\right|_{e,3} - k_4 A_4 \left.\frac{dT}{dx}\right|_{e,4} \quad (14)$$

The gradient terms for A1 and A2 in equation 14 are evaluated using the solution to the convection-diffusion equation and are given by equations 15 and 16, respectively. This leaves only terms for the inactive areas of the envelope, A3 and A4, to be evaluated. Since these areas are not affected by infiltrating air, their conduction flux terms remain constant. The product of the gradient term and thermal conductivity in areas 3 and 4 of the envelope will be represented by a constant as given by equations 17 and 18, respectively. Finally, the evaluated terms are placed back into equation 14 to give a new relation for the total conduction flux, equation 19.

$$\left.\frac{dT}{dx}\right|_{e,1} = (T_i - T_o)\frac{Pe_1}{L}\frac{1}{e^{Pe_1} - 1} \quad , \quad \left.\frac{dT}{dx}\right|_{e,2} = (T_o - T_i)\frac{Pe_2}{L}\frac{e^{Pe_2}}{e^{Pe_2} - 1} \quad (15), (16)$$

$$q_{0,3} = k_3 \left.\frac{dT}{dx}\right|_{e,3} \quad , \quad q_{0,4} = -k_4 \left.\frac{dT}{dx}\right|_{e,4} \qquad (17),\ (18)$$

$$Q_{cond} = k_1 A_1 (T_i - T_o) \frac{Pe_1}{L} \frac{1}{e^{Pe_1} - 1} + k_2 A_2 (T_i - T_o) \frac{Pe_2}{L} \frac{e^{Pe_2}}{e^{Pe_2} - 1} + A_3 q_{0,3} + A_4 q_{0,4} \qquad (19)$$

The term Q_o represents the total energy flux across the building envelope when there is no infiltration, i.e., pure conduction. For the envelope in this analysis, Q_o is represented as the sum of four constant terms as shown in equation 20. It is assumed that there is a linear temperature profile through the wall and the heat flux obeys Fourier's law for heat conduction (8). This allows the conduction heat flux terms in the wall with no infiltration, q_o, to expressed as in equation 21.

$$Q_0 = A_1 q_{0,1} + A_2 q_{0,2} + A_3 q_{0,3} + A_4 q_{0,4} \qquad (20)$$

$$q_{0,1} = k_1 \left.\frac{dT}{dx}\right|_{e,1} = k_1 \frac{T_i - T_o}{L} \qquad (21)$$

4.4 Heat Recovery Factor

The information from the previous sections can be used with the definition of the heat recovery factor to provide a new relationship for this quantity as given by equation 22. The heat recovery factor is a function of the wall thermal conductivity, active area, wall thickness, and Peclet number for both the infiltrating and exfiltrating walls.

$$e = 1 - \frac{k_1 A_1 \frac{Pe_1}{e^{Pe_1} - 1} + k_2 A_2 \frac{Pe_2 e^{Pe_2}}{e^{Pe_2} - 1} - (k_1 A_1 + k_2 A_2)}{m c_p L} \qquad (22)$$

The next step is to recast the Peclet number in terms of quantities that are meaningful for this application. Equation 23 shows the definition of the Peclet number. The velocity, u, in equation 23 is replaced by the relation shown in equation 24 where m is the mass flow rate of leaking air, r is the air density, and A is the effective area. The thermal conductivity, k, is replaced by the U-value for the wall via equation 25, which makes use of the relation for conduction given by equation 21. This step replaces the micro-scale material property, k, with the macro-scale effective U-value for the composite wall system. The Peclet number is transformed into a dimensionless flow rate, a, using effective values characteristic to the system as shown in equation 26.

$$Pe = \frac{ruL}{k / c_p} \quad , \quad u_i = \frac{m}{rA_i} \qquad (23),\ (24)$$

$$U_i = \frac{q_{o,i}}{\Delta T} = \frac{k_i}{L} \qquad , \qquad a_i = \frac{mc_p}{U_i A_i} \qquad (25), (26)$$

Using the relations in equations 23-26, a new expression is created for the heat recovery factor and is given by equation 27. Equation 27 shows that the heat recovery factor is a function only of the dimensionless flow rate, a_i, for the infiltrating and exfiltrating walls. When presented in this form the symmetry between infiltration and exfiltration is apparent.

$$e = -\frac{1}{e^{a_1}-1} - \frac{1}{e^{a_2}-1} + \frac{1}{a_1} + \frac{1}{a_2} \qquad (27)$$

One last change is made in the expression for the heat recovery factor, a simplification for ease of use. A value is determined for the non-dimensional flow rate for the entire structure, denoted as a_o, using the overall U-value and the total surface area of the building, denoted as A, as shown in equation 28. Both a_1 and a_2 can now be expressed in terms of a_o and the unknown effective areas can be extracted into separate parameters as area ratios weighted by the U-values, as equations 29 and 30 show. The final form of the expression for the heat recovery factor is given by equation 31. It shows that the heat recovery factor for a given envelope depends on the UA of the building and the infiltration rate, which appear as a_o, and the effective areas for infiltration and exfiltration, which appear as the effective area ratios, f_1 and f_2.

$$a_o = \frac{mc_p}{UA} \qquad (28)$$

$$f_1 = \frac{a_o}{a_1} = \frac{U_1 A_1}{UA} \qquad , \qquad f_2 = \frac{a_o}{a_2} = \frac{U_2 A_2}{UA} \qquad (29), (30)$$

$$e = -\frac{1}{e^{a_o/f_1}-1} - \frac{1}{e^{a_o/f_2}-1} + \frac{f_1 + f_2}{a_o} \qquad (31)$$

4.5. Comparison of Mathematical Model with CFD Results

Predictions of the heat recovery factor made with the mathematical model, equation 31, are now compared to values determined from CFD simulations. In these comparisons, the area ratios in the model, f_1 and f_2, are adjusted to provide the best overall agreement as determined by a least-squares fit. The ratios are given equal values here because the infiltrating and exfiltrating walls used in the CFD simulations were symmetric.

Figure 5 shows heat recovery values for the walls with a high/low hole configuration determined from 2D and 3D CFD simulations and the model. The value for the area ratio was adjusted to give the best agreement, which, for this case, was found to be 0.33, or 33 percent of the wall area. The model predictions show fairly good agreement with CFD results, but do

not match exactly. Better agreement would occur if the model predictions were slightly lower at small leakage rates and slightly higher at large leakage rates.

Figure 6 shows heat recovery values for the walls with a straight through hole configuration determined from 2D and 3D CFD simulations and the model. For this case, the best agreement was achieved with a value of 0.18 for the area ratio, or 18 percent of the wall area. Agreement is good, but, as before, agreement would be better if the model predictions were slightly lower at small leakage rates and slightly higher at large leakage rates.

The results in figures 5 and 6 suggest that our simple model does not capture the full physics of the problem. While the trend is generally correct, the model predictions decrease faster at high flow rates than the CFD data does. Some of the CFD results suggest that part of the heat recovery occurs in the thermal boundary layers on each side of the wall and part occurs within the wall. For example, cool infiltrating air falls along the inner surface of the wall reducing the conductive heat loss. Also, some of the air sucked into the leak from the external boundary layer will be at a higher temperature (a smaller overall temperature difference) and will mitigate the infiltration load. This effect would imply that even with no heat exchange within the wall itself there would be some heat recovery. We believe these effects contribute to heat recovery, but they are not explicitly included in our model.

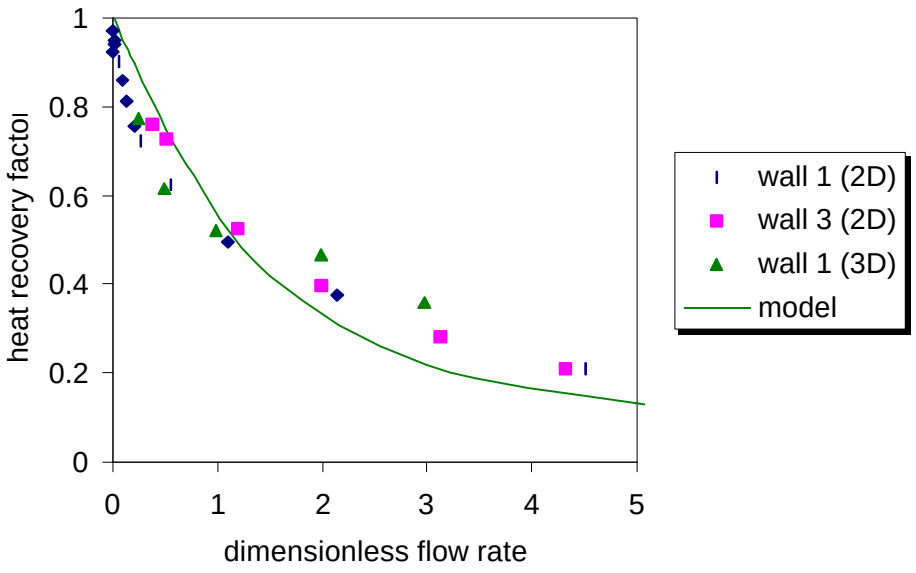

Figure 5: Heat recovery factor for walls with a high/low hole configuration (insulated and empty wall cavities) determined from CFD simulations and the simplified model using a constant area ratio (*f=0.33*).

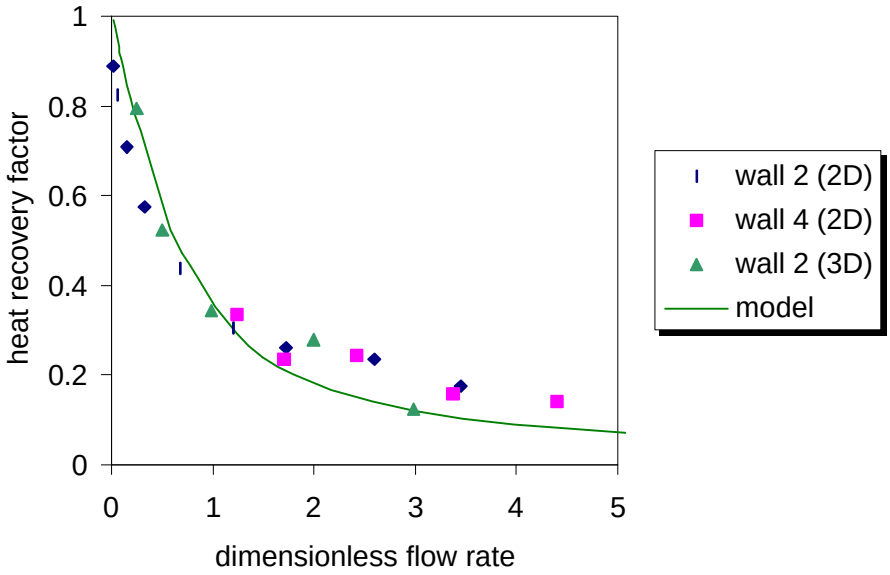

Figure 6: Heat recovery factor for walls with a straight through hole configuration (insulated and empty wall cavities) determined from CFD simulations and the analytical model using a constant area ratio (*f=0.18*).

5. Conclusions

In this study, CFD simulations were used to examine the fundamental physics of the infiltration heat recovery process. Results were found to compare well (within about 10 percent) with limited published laboratory data corresponding to one of the leakage scenarios examined. Also, a simple, robust macro-scale mathematical model was developed that can accurately predict the heat recovery factor for air infiltrating through building walls when supplied with the proper input. The required inputs are the building U-value, the leakage rate, and an effective area for infiltration and exfiltration. The effective areas were determined here for specific leakage geometries through comparison with CFD data.

These results show the potential importance of infiltration heat recovery. The extent of heat recovery was found to be dependent on the leakage path geometry, infiltration flow rate, and wall construction. In some cases with low infiltration rates and long leakage paths, the heat recovery can be substantial, well over 80 percent. In these cases, the conventional method would over-predict the extra heating load due to infiltration. According to these findings, under typical leakage conditions for most residential buildings ($a_o \leq 1$) the heat recovery could be around 40 percent.

All possibilities have not been examined in this study, but it is clear that some modification could be made to the conventional method for prediction of infiltration energy loads to increase its accuracy. The model for infiltration heat recovery presented in this paper could easily be incorporated into whole-building energy analysis programs to provide improved predictions for the energy impact of steady-state infiltration.

References

1) Bhattacharyya, S., Claridge, D. E. (1995) "The energy impact of air leakage through insulated walls", *Transactions of the ASME,* Vol. 112, pp. 132-139.

2) Buchanan, C.R., Sherman, M. H. (1998) "Simulation of Infiltration Heat Recovery", 19th AIVC Annual Conference, Oslo, Norway, September, 1998.

3) Burns, P. J., Chow, L. C., Tien, C. L. (1977) "Convection in a vertical slot filled with porous insulation", *Int. J. Heat Mass Transfer*, Vol. 20, pp. 919-926.

4) Caffey, G. E. (1979) "Residential air infiltration", *ASHRAE Trans.*, Vol. 85, pp. 41-57.

5) Claridge, D. E., Liu, M. (1996) "The measured energy impact of infiltration in an outdoor test cell", *Transactions of the ASME,* Vol. 118, pp. 162-167.

6) Claridge, D. E., Bhattacharyya , S. (1990) "The measured impact of infiltration in a test cell", *J. Solar Energy Engineering*, Vol. 117, pp. 167-172.

7) Kohonen, R., Virtanen, M. (1987) "Thermal coupling of leakage flow and heating load of buildings", *ASHRAE Trans*., Vol. 93, pp. 2303-2318.

8) Mills, A. F. (1992) *Heat Transfer*. Irwin, Burr Ridge, Illinois

9) "NIST estimates nationwide energy impact of air leakage in U. S. buildings" (1996) *J. Research of NIST*, Vol. 101, No. 3, p. 413.

10) Persily, A. (1982) "Understanding air infiltration in homes", Report PU/CEES No. 129, Princeton University Center for Energy and Environmental Studies, February, p. 335.

11) Sherman, M., Matson, N. (1993) "Ventilation-Energy liabilities in U.S. dwellings", 14th AVIC Conference: Energy impact of ventilation and air infiltration, Copenhagen, September 21-23, Proceedings, pp. 23-41.

12) Versteeg, H. K., Malalasakera, W. (1995) *Introduction to Computational Fluid Dynamics.* Longman Scientific & Technical, New York.